NUMERICAL AND EXPERIMENTAL DETERMINATION OF STRESS INTENSITY FACTORS IN A 2o kHz RESONANCE SYSTEM

A. F. Blom[+], A.Hadrboletz[++] and B.Weiss[++]

To determine the threshold stress intensity factors for fatigue crack growth it seems advantageous to adapt high frequency resonance test methods (up to 2o kHz) to reduce the required test time .However, in such techniques the initial computation of the stress intensity factor did not incorporate the peculiarities of a resonance system. Dynamic stress intensity factors in a 2o kHz resonance system are determined by means of a direct integration dynamic finite element analysis and experimentally with a modified compliance test method. The effects of closing and opening of the crack tip at tests performed at R=-1 are outlined. These findings were applied to the evaluation of threshold data of Cu- and Al-alloys.

INTRODUCTION

During the last years increasing interest appeared in methods for measurements of crack growth phenomena at extremely low growth rates and for the determination of threshold values of crack growth under cyclic loading in various environments for a variety of pure metals and technical alloys (1).

To reduce the experimental effort for such types of measurements test-procedures have been suggested which employ increased cyclic frequencies e.g. $1o^3$ to $1o^4$ Hz (2,3). In particular, test methods have been developed which involve the cyclic loading of suitably dimensioned specimens at a resonance frequency of approximately 2o kHz. A review of the application of these 2o kHz resonance methods for the determination of crack growth rates (da/dN) down to $1o^{-13}$m/cycle and of threshold values (ΔK_{Th}) has recently been presented (2). For the computation of stress intensity factors K from the 2o kHz-test results initially the same correction functions have been applied in the literature to static tests eq. 1 (4) without taking into account the peculiarities of the

$$K = \sigma_\infty \sqrt{\pi a}\, Y\left(\frac{2a}{B}\right) \quad \ldots\ldots \quad (1)$$

+) Depart.of Aeronautical Structures and Materials, Royal Inst. of Technology, Stockholm, Sweden and Structures Department, The Aeronautical Research Inst.of Sweden

++) Institut für Festkörperphysik, University of Vienna, Austria

resonance test procedure. Initial attempts to account for the effects of the presence of a crack on the resonance behaviour of a specimen excited to longitudinal vibrations have been described in Ref.(5). More recently, dynamic stress intensity factors computed by finite element methods have been published by Hoffelner et al. (6) who limit the validity of their results to loading conditions R=0.

The aim of the present study was to determine the dynamic stress intensity factors and the appropriate correction function Y (2a/B) first by means of a finite element computation procedure and secondly by measurements using a modified compliance test method. The test conditions involved longitudinal resonance vibrations at 2o kHz of a center-notched flat plate specimen for a stress ratio of R = -1. The validity of this approach is demonstrated by test results obtained from specimens of pure Cu and an Al-alloy (Al-2o24).

TEST METHOD

The experimental test system used for these measurements has been described previously (5,7,21). The mechanical resonance system operating at 2o kHz consists of a piezo-electric transducer coupled to mechanical amplitude transformers and half-wave length coupling pieces. The half-wave length dimensioned specimen is suitably coupled to this mechanical resonance system and excited to longitudinal push-pull vibrations. The strain distribution along the length of the specimen is sinusoidal with a maximum of the strain occuring in the middle of the specimen, Fig.1. In the particular test system the specimen is cyclically loaded under zero mean stress (R = -1). The strain distribution in the resonance specimen is compared with that of a conventionally loaded specimen in Fig 1a and 1b, respectively.

EXPERIMENTAL K- CALIBRATION

From the well known relationship for the crack extension force G (8)

$$G = \frac{1}{2D} F^2 \frac{dC}{d2a} \quad \ldots\ldots\ldots\ldots (2)$$

one can obtain with

$$G = (1-\nu^2) \frac{K^2}{E} \quad \ldots\ldots\ldots (3)$$

the following expression for the function $Y(\frac{2a}{B})$ as given in eq.4.

$$\left[Y\left(\frac{2a}{B}\right)\right]^2 = \frac{ED}{(1-\nu^2)\frac{2a}{B}\cdot\pi} \cdot \frac{dC}{d(\frac{2a}{B})} \quad \ldots\ldots (4)$$

To determine Y (2a/B) the compliance C

$$C = \frac{V}{F} \quad \ldots\ldots\ldots\ldots\ldots\ldots (5)$$

was measured using specimens of constant width containing centered saw cuts of various lengths to simulate center cracks (9). The experimental procedure to measure the crack opening

displacement of a center-notched 2o kHz resonance specimen was similar to that described by Schmidt and Paris (2) and Gan and Weertman (1o) for conventional specimens. A miniature strain gauge (HBM type LY 11/0,6/12o) with an active gauge section (l= o,6 mm) smaller than the width of the saw-cut (0,8 mm) was placed over the center of the saw-cut (Fig.2). The crack opening displacement was then calculated from the measured strain signal ε_1

$$v = l \cdot \varepsilon_1 \quad \ldots\ldots (6)$$

The direct determination of the applied force or stress is not possible in a resonance specimen (5). It can be calculated under certain assumptions e.g. from the displacement amplitude U_o at the ends of the vibrating specimen or from the strain in the center of the specimen, Fig.1. In the present investigation, however, the stress amplitude σ_∞ was deduced from the measured strain ε_2 in the plane of the saw-cut. As a result of the decreased cross-section in the plane of the crack (saw-cut) an excess of strain occurs in comparison to a defect-free specimen. The distribution of this excess strain along the length of the specimen was measured with a multisection strain gauge (Fig.2) (HBM type KY 21, 1o sections 1o mm total length). The measurements were carried out both with specimens containing a centered saw-cut and with specimens containing symmetrical cracks emanating from a spark - machined center notch. In the latter case the loading amplitudes were chosen sufficiently high to ensure that K_{max} is greater than K_{op} (11).

The results of this investigation are shown in Fig.2 for a specimen containing a saw-cut of the dimensions 2a/B = 0,47. It can be seen that the local increase in strain corresponds precisely to the decrease in cross-section as compared with an unnotched specimen. The strain increase is distributed over an area large enough to be recorded with the miniature strain gauge of an active length of 0.6 mm. Therefore in this case the force F can be expressed as

$$F = E\varepsilon_2 DB \quad \ldots\ldots\ldots (7)$$

The strain gauges 2 and 7 were applied to monitor the occurence of transverse vibrations.

The experimental determination of the function Y(2a/B) was deduced from a plot of ε_1 vs ε_2 values obtained from copper specimens (B = 15 mm) containing saw-cuts of various lengths, Fig.3a. Since ε_1 is proportional to v and ε_2 is proportional to F the value of C can be obtained as a function of 2a/B by re-plotting the data of Fig 3a as shown in Fig 3b. Invoking the relationship of eq.4 the correction function Y(2a/B) follows from the curve shown in Fig.3b and is shown in Fig. 3c for a center notched specimen loaded under R =-1.Similar results were obtained for center cracked specimens within a scatterband of 5%.

Measurements with other metals and alloys (e.g. Cu of different degrees of strain hardening, Al-alloy 2o24) indicated that the determined relationship is essentially independent of the specimen material.

For the determination of ΔK center cracked specimens were used. Hereby the strain distribution along the specimen was measured since there could be differences in the response in tension and compression, respectively. These measurements were performed in a similar way as described for the specimens containing a central saw cut, Fig.2. The experimental results obtained from these two types of specimens revealed that the local increase in strain is less in the specimen containing the crack than in the specimen containing the saw-cut.

This observation may be explained by the fact that in a specimen containing a narrow crack the contribution to the local increase in strain is different in the tension and compression half cycle as can be shown schematically in Fig.4a. In the compression phase the cross section of the specimen is reduced essentially only by the size of the initial notch (introduced by spark-machining), while in the tension phase the remaining cross-section is given by the size of the initial notch added to the length of the cracks.

The strain distribution was determined for different crack lengths. As an example the strain distribution in a specimen containing a crack of $2a/B=0.47$ is shown in Fig. 4a. From the above measurements a further correction function Φ was determined as plotted in Fig. 4b for different ratios of $2a/B$ and $2\varrho/B$.

DYNAMIC FINITE ELEMENT ANALYSIS

Although the test specimen is subjected to a non-symmetrical displacement the lowest symmetrical mode is achieved in the experimental setup. In the numerical model, Fig.5, a coupling element is used to achieve the symmetrical mode. The properties of the coupling element is derived in Ref.(12) where also a detailed description of the FEM-analysis is given. Since the specimen contains a crack which alternatingly opens and closes the problem is nonlinear. For this reason a mode superposition analysis is difficult to perform. Thus, a direct time integration technique is used. The specimen is studied at its lowest eigenfrequency. Therefore an implicit method ought to be used.

The most known implicit direct integration method is probably Newmark's constant-average-acceleration scheme (13). This technique does, however, lack numerical dissipation i.e. the energy in the system is preserved why the false eigenmodes introduced by the chosen element mesh are not damped but superposed to the physical modes. The new α-method by Hilber (14,15, 16) does allow numerical dissipation. Therefore this technique is used here. The algorithm is implemented in the finite element code GENFEM (17,18,19).

The opening and closing of the crack during each load cycle is numerically taken into account by means of linear constraints. The displacement of one side of the crack surface u_1 is written as the sum of the displacement of the other side of the crack surface u_2 plus the crack opening δ. When the force over the crack is positive δ is let free and the crack will open. When the force over the crack is negative δ is prescribed to zero and the two crack surfaces follow each other. The finite element mesh is shown in Fig.5. Linear constraints are used where the

mesh is refined so that continuity is preserved between elements. Isoparametric 8-noded elements are used and to achieve the expected $r^{-1/2}$-singularity at the crack tip the elements adjacent to the crack tip are degenerated into triangles with the mid-side node in the quarter point (2o). Stiffness and damping properties are chosen so that the eigenfrequency for the system coincides with the eigenfrequency of the test specimen alone. The calculated eigenfrequency of the system is f = 17125 Hz whereas measurements on the test specimen give f = 17115 Hz.

The timestep in the direct integration is chosen to 1/2o of the period for the lowest eigenmode, i.e. $\Delta t = 1.1/f = 2.92\ 1o^{-6}$s. The transient response is damped to less than 2% in three periods. All calculations are performed after five periods to ensure stationary conditions. Each calculation thus consists of 1oo time-steps.

To find out how much the dynamical response of the specimen is affected by the opening and closing of the crack three sets of calculations were performed. The specimen was analysed without any crack at all, i.e. a solid specimen, then it was analysed with a crack but without the control of opening and closing discussed above, i.e. R > 0, and finally it was fully analysed with controlled opening and closing of the crack, i.e. R = -1.

Results from such calculations are shown in Table 1 for two different crack lengths, 2a/B = o,25 and 2a/B = o,5. It can be seen that the influence of the crack on the dynamical response is small as the mass-forces mainly occur in the ends of the specimen where the acceleration is largest. Comparisons with static FEM calculations show a negligible difference. For the case with a short crack, 2a/B = o,25, we find that the influence of the opening and closing on the dynamical response is negligible whereas for larger cracks, 2a/B = o,5, there is indeed a significant difference between tensile and compressive response.

TABLE 1 - Dynamical finite element results.

		massive specimen	2a/B = 0,25 R=0	2a/B = 0,25 R=-1	2a/B = o,5 R=0	2a/B = o,5 R=-1
U_o	µm	19,85	19,92	19,9o	2o,21	2o,o3
ϵ_{max}	o/oo	o,395	o,4o7	o,4o4	o,465	o,48o
ϵ_{min}	o/oo	-o,395	-o,4o7	-o,399	-o,465	-o,4oo
δ_{max}	µm	-	2,68	2,68	6,5o	6,34
δ_{min}	µm	-	-2,68	o	-6,52	o

DISCUSSION

Various correction functions obtained by different procedures are

plotted in Fig. 6. Curve 1 is valid for a semi-infinite strip (4) and shows too high values for specimens used in ultrasonic fatigue testing. Curve 2 is obtained by the FEM technique described above for an Al-2o24 specimen with a length to width ratio of 1o. The curve is valid for both the static and the dynamic case since the difference is always less than 2%. Curve 3 is obtained, by the experimental technique previously discussed, for Cu-specimens with a length to width ratio of about 6. Allowing for an experimental error of 5% and considering the different length to width ratios we get a fairly good agreement between curves 2 and 3. Curve 4 shows a dynamic FEM solution for a Cu specimen with a length to width ratio of 4.6 reported in Ref. (6). These results were obtained with a stress ratio R=0 whereas the experimental results shown in curve 3 were obtained with R = -1. Also here a good agreement can be seen.

For the computation of σ_∞ from reading of a strain gauge applied at the edge of the specimen in the plane of the crack, the correction function $Y(\frac{2a}{B})$ to account for the finite specimen width has to be multiplied by a further function Φ (2a/B, 2ς/B). These functions are shown as solid lines in Fig.4b. They have to be employed since the experimental strain measurements at a test frequency of about 2o kHz give arithmetic mean values of tensile and compressive amplitudes only. As can be seen from the FEM-results in Table 1 the strain value in tension is not equal to the value of the strain in compression. From these strain data it may be deduced that the measured strains for 2a/B=0.5 are about 9% too low. For 2a/B ratios below 0.25 there is no such difference and the dashed line in Fig.4b shows the assumed correction function. The differences between the dashed and the solid lines in Fig.4b may be due to the reasons outlined above and also the fact that the machined notch is not modelled in the FEM-analysis.

In Table 2 various threshold values ΔK_{th} determined by the 2o kHz resonance method are listed. ΔK_{th} values are computed with the correction functions determined in the present investigation and are compared with the initial computation method cited in (5).

The approximate correction function applied for ΔK computation in previous publications (1,5) has been found to overestimate the effects of the reduced cross-section, resulting in a maximum deviation of 2o% from the values computed by the method described above.

The evaluation of ΔK values for 2o kHz-resonance specimens from measurements of the displacement amplitudes at the ends of the specimens appears questionable in view of the rather complex distribution of the strain in the plane of the crack caused particulary by the differences in excess strain during the tension and compression half cycles.

In our investigation we have extended the determination of the correction function Y(2a/B) only up to a value of $2a/B \leq 0.5$. The reason for this limitation is the excitation of vibrations at higher harmonics. The amplitude of which may exceed negligible values if the crack grows to dimensions exceeding approximately 1/2 of the specimen width. In contrast to center cracked specimens we found that in edge cracked specimens transverse

TABLE 2 - Threshold values for different materials

material	L/B	B(mm)	2ϱ/B	2a(mm)	$\varepsilon=\frac{\varepsilon_{max}+\varepsilon_{min}}{2}$	E(MPa)	ΔK_{Th} (MPa$\sqrt{m}$) Ref.(5)	this paper
Al 2024 T3	10	15	0,16	3,62	$4,3\ 10^{-4}$	72500	1,85	2,2
				4,02	$4,1\ 10^{-4}$		1,80	2,2
				4,62	$3,75\ 10^{-4}$		1,70	2,1
Cu (450°C,2h)	6	14	0,15	4,56	$2,7\ 10^{-4}$	126000	2,10	2,6
				5,10	$2,5\ 10^{-4}$		1,95	2,5
				5,20	$2,5\ 10^{-4}$		1,96	2,5
Cu (650°C,4h)	6	14	0,15	3,58	$2,7\ 10^{-4}$	126000	1,98	2,4
				4,26	$2,5\ 10^{-4}$		1,90	2,4

plate-vibrations are excited. These plate vibrations considerably affect the accuracy of the determined ΔK values already at a/B≈ 0,3 as has been already pointed out by Hoffelner (6).

The authors like to thank Prof.R.Stickler and Dr.R.Glemberg for helpful discussion.

SYMBOLS USED

2a ..... crack length
B ..... specimen width
C ..... compliance
D ..... specimen thickness
E ..... Young's modulus
F ..... force
G ..... crack extension force
K ..... stress intensity factor
ΔK ..... $(K_{max}-K_{min})$ R>0
K_{max} R≤0.
l ..... active gauge length
L ..... specimen length
R ..... $\sigma_{min}/\sigma_{max}$
u ..... displacement
U_o ..... displacement amplitude
v ..... crack opening
Y(2a/B). correction function
δ ..... u_1-u_2
ε ..... strain amplitude
σ_∞ ..... applied stress
2ϱ ..... machined notch size
Φ ..... correction function
ν ..... Poisson's ratio

REFERENCES

1. Bäcklund,J.,Blom,A.F. and Beevers,C.J., 1982,"Fatigue Thresholds, Fundamentals and Engineering Applications", EMAS, U.K.

2. Schmidt,R.A. and Paris,P.C., 1973, "Progress in Flaw Growth and Fracture Toughness Testing", ASTM STP 536, USA

3. Wells J, et al., "Fatigue and Corrosion Fatigue up to Ultrasonic Frequencies", 1981, Proceedings of the 1st International Symposium, Seven Springs, USA

4. Tada,H., Paris,P.C.,and Irwin,G.,1973, "The Stress Analysis of Cracks Handbook", Del Research Corp., USA

5. Weiss,B.,Stickler,R.,Bildstein,H.,Pfaffinger,K.,and Femböck, J., 198o, Metall, 7, 636

6. Hoffelner,W.and Gudmundson,P.,1982, Engineering Fracture Mechanics, 16, 365

7. Willertz,L.E.,198o, Internat.Met.Rev., 2, 65

8. Broek,D.,1978, "Elementary Engineering Fracture Mechanics", Sijthoff and Noordhoff, Netherlands

9. Schwalbe,K.H.,198o, "Bruchmechanik metallischer Werkstoffe", Carl Hanser Verlag, München, GFR

1o. Gan,D.and Weertman,J.,1981, Eng.Fract.Mech.,15, 87

11. Hadrboletz,A., unpublished results

12. Glemberg,R.,Blom,A.F. and Bäcklund,J.,: FEM-analysis of Dynamic Stress Intensity Factors, to be published

13. Newmark,N.M., 1959, J.Engng.Mech.Div., ASCE, 85, EM 3, 67

14. Hilber,H.M.,1976, EERC Report No.76-29, Univ.of California, U.S.A.

15. Hilber,H.M.,Hughes,T.J.R. and Taylor,R.L.,1977, Earthg. Engn.Struct.Dyn.,5, 283

16. Hilber,H.M. and Hughes,T.J.R.,1978, Earthg.Engng.Struct. Dyn., 6, 99

17. Wennerström,H.,Glemberg,R.and Petersson,H.,1979, GENFEM-3, Users Manual, Publication 79:4, Chalmers University of Technology, Sweden

18. Wennerström,H. and Petersson,H.,1979, GENFEM-3,Verification Manual, Publication 79:5, Chalmers University of Technology, Sweden

19. Glemberg,R.,:Addendum to the GENFEM-3 Users Manual, The Hilber, Hughes α-method- In preparation

2o. Barsoum,R.S., 1976, Int.J.Numerical Methods in Engn, 1o, 197

21. Stickler,R. and Weiss,B. in Ref.3

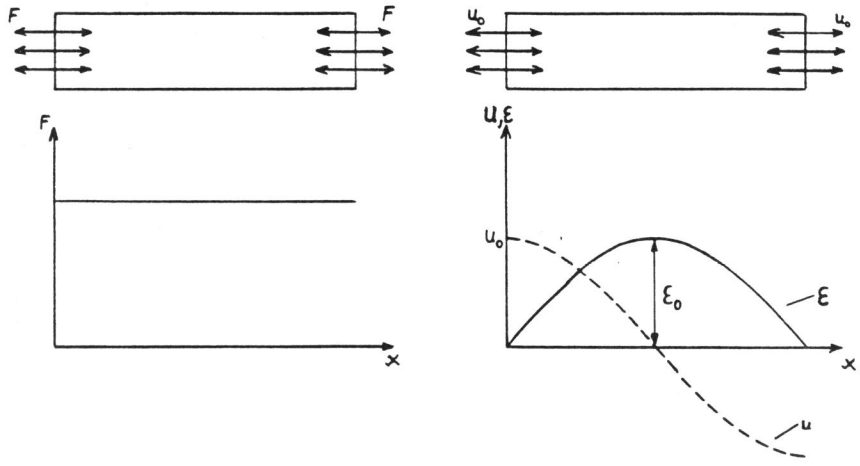

a) conventional

b) resonance
ε....strain amplitude
u....displacement amplitude

Fig.1 Loading conditions for center notched specimens tested by conventional and resonance methods

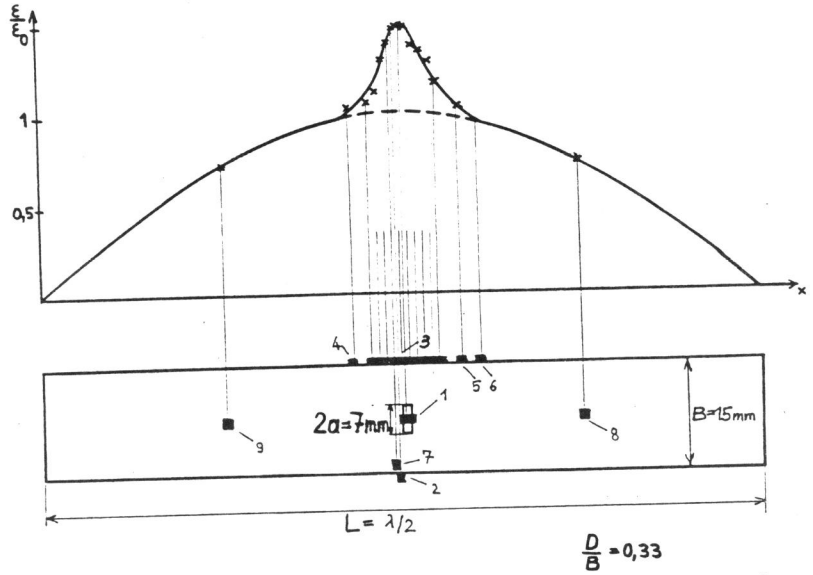

Fig.2 Measured strain distribution along a resonance specimen with a saw cut

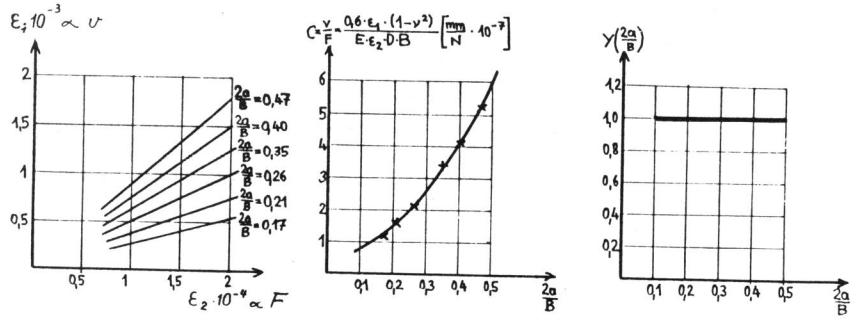

Fig.3 Experimental determination of the correction function Y(2a/B)

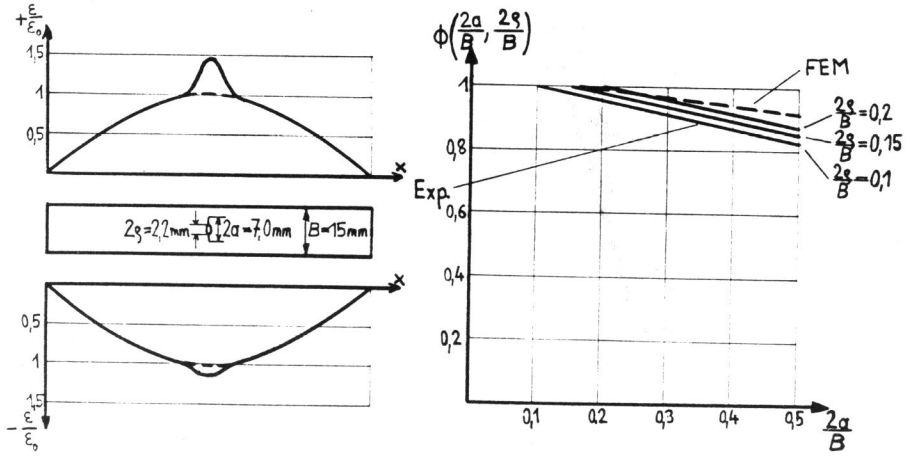

Fig.4 Measured strain distribution and correction function Ø for center cracked specimens

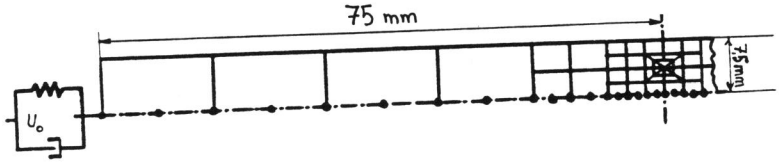

Fig.5 Finite Element model

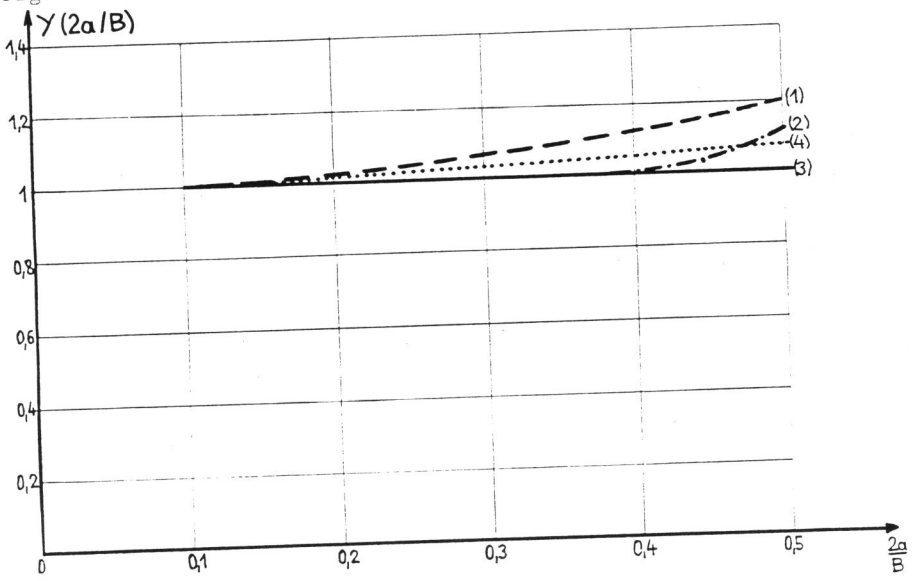

Fig.6 Various correction functions Y(2a/B)